eXPRESS Polymer Letters Vol.9, No.10 (2015) 916–931
Available online at www.expresspolymlett.com
DOI: 10.3144/expresspolymlett.2015.83

Effect of surface modified TiO_2 nanoparticles on thermal, barrier and mechanical properties of long oil alkyd resin-based coatings

T. S. Radoman[1], J. V. Džunuzović[2], K. T. Trifković[1], T. Palija[3], A. D. Marinković[4], B. Bugarski[4], E. S. Džunuzović[4]*

[1]Innovation center, Faculty of Technology and Metallurgy, University of Belgrade, Karnegijeva 4, 11120 Belgrade, Serbia
[2]Institute of Chemistry, Technology and Metallurgy (ICTM), Center of Chemistry, University of Belgrade, Studentski trg 12–16, 11000 Belgrade, Serbia
[3]Faculty of Forestry, University of Belgrade, Kneza Višeslava 1, 11000 Belgrade, Serbia
[4]Faculty of Technology and Metallurgy, University of Belgrade, Karnegijeva 4, 11120 Belgrade, Serbia

Received 18 February 2015; accepted in revised form 25 May 2015

Abstract. Novel soy alkyd-based nanocomposites (NCs) were prepared using TiO_2 nanoparticles (NPs) surface modified with different gallates, and for the first time with imine obtained from 3,4-dihydroxybenzaldehyde and oleylamine (DHBAOA). Unmodified and surface modified anatase TiO_2 NPs were characterized by transmission electron microscopy (TEM), X-ray diffraction (XRD), Fourier transform infrared spectroscopy (FTIR) and ultraviolet-visible (UV-Vis) spectroscopy, while the amount of adsorbed ligands was calculated from thermogravimetric analysis (TGA) results. Surface modification of TiO_2 NPs was confirmed by FTIR and UV-Vis spectra. The influence of the TiO_2 surface modification on the dispersion of TiO_2 NPs in alkyd resin, thermal, barrier and mechanical properties and chemical resistance of alkyd resin/TiO_2 NC coatings was investigated. The obtained results revealed that glass transition temperature of all investigated NCs is lower than for pure resin, that the presence of TiO_2 NPs surface modified with gallates had no significant influence on the thermooxidative stability of alkyd resin, while TiO_2-DHBAOA NPs slightly improved alkyd resin thermooxidative stability. Also, the presence of surface modified TiO_2 NPs improved barrier properties, increased stress and strain at break and hardness and chemical resistance and decreased modulus of elasticity and abrasion resistance of alkyd resin.

Keywords: *thermal properties, alkyd-based coatings, TiO_2 nanoparticles, surface modification, mechanical properties*

1. Introduction

Alkyds are the most widely used synthetic resins due to their relatively low cost, compatibility with other polymers and various interesting properties which are highly desirable for the application in paint industry. The versatility of alkyd resins originates from the fact that their properties such as drying time, gloss retention, anticorrosion, mechanical, thermal and barrier properties, durability, flame retardancy, water and chemical resistance and adhesion can be easily tailored and improved by simple changing the ratio and type of the applied reactants, the oil length or by modification of alkyd resins with different reactive compounds [1]. Alkyd resins are obtained by polycondensation of polyol (glycerol, trimethylolpropane, pentaerythritol, etc.) with dicarbonic acid or its anhydride derivative in the presence of fatty acids or oil of synthetic or natural origin (soya bean oil, linseeds oil, sunflower oil, castor oil, etc.). The content of oil, which corresponds to the oil length, has significant influence on the properties of alkyd resins [1, 2]. Depending on the composition of the

*Corresponding author, e-mail: edzunuzovic@tmf.bg.ac.rs

fatty acids used for the synthesis, alkyd resins can be cross-linked (dried) using either oxidative drying (unsaturated fatty acids) or non-oxidative drying (saturated fatty acids) mechanism [2–4].

Alkyd resins based on non-toxic, biodegradable, multifunctional, low cost, physically and chemically stable and eco-friendly renewable resources such as vegetable oils show properties comparable with properties of products based on petroleum, and therefore have found their industrial application in paints and surface coatings [5–19]. Especially interesting low cost vegetable oil is soy bean oil, which has balanced composition of unsaturated and saturated fatty acids and it can reduce yellowing and oxidative degradation of resin [2, 16–19]. Araujo *et al*. [16] have shown that anticorrosive properties of alkyd paints prepared with soy bean oil are similar to the anticorrosive properties of alkyd resins synthesized using linseed oil, but water vapor and ions permeability in freestanding film, as well as adhesion loss, depend on the type of pigment and vegetable oil used in the formulation of alkyd resins. By comparing properties of short oil-modified alkyd resins prepared using soy bean, corn, rice bran, sunflower and dehydrated castor oil, it was revealed that soy bean based alkyd resin show the best sea water resistance [17]. Nalawade *et al*. [19] have used modified soy bean oils as reactive diluents for the preparation of long oil alkyd resin, which had significantly reduced viscosity.

Different commercial, micro-sized, inorganic pigments are usually included in alkyd resin formulations, and their presence can improve mechanical, optical and anticorrosive properties of the coatings [20, 21]. However, due to their micro-sizes, densities different from the density of alkyd resins, and other various effects, sedimentation of pigments occurs, leading to different problems considering final alkyd-based coatings (viscosity changes, covering power deterioration, poor adhesion, loss of optical transparency, low scratch and impact resistance, delamination, reduction of the storage time, etc.) [22]. Sedimentation issue can be avoided if small quantities of nano-sized pigments are used in the alkyd resin formulations instead of micro-sized ones. The main advantages of the application of nanoparticles (NPs) for the preparation of polymer nanocomposites (NCs) are high surface to volume ratios and high interfacial reactivity of NPs and properties which are significantly different from the properties of their bulk counterparts and micro- and macro-additives [23]. By adequate surface modification of NPs it is possible to enable uniform distribution of NPs through the polymer matrix and better interaction with polymer in order to achieve significant improvement of properties of polymer materials with simultaneous decrease of the final product price [24, 25]. The influence of different nano-sized pigments on the properties of alkyd-based NCs was extensively investigated in the literature [26–37]. It has been shown that application of zinc oxide (ZnO) as nano-sized pigment improves mechanical and thermal properties [26] and corrosion resistance [27] of alkyd-based coatings. Furthermore, the presence of titanium dioxide (TiO_2) NPs affects the rheological properties of alkyd resin [28], improves corrosion resistance [29, 30] and hardness of alkyd coatings [29], and can be applied for the preparation of coatings with antibacterial properties [31]. Also, hematite (Fe_2O_3) NPs are proven to be useful nano-pigment which enhances mechanical and UV blocking properties [32] and corrosion resistance [32, 33] of alkyd-based waterborne coatings. The presence of nano-ferrite (Fe_3O_4) in soy alkyd coating improved thermal stability, physico-mechanical properties and corrosion resistance [34]. The addition of aluminum oxide (Al_2O_3) nano-sized pigment into the alkyd coatings improved its corrosion [35, 36] and UV resistance and mechanical properties, without altering the optical clarity of the prepared coating [36]. Alkyd paint prepared using molybdenum oxide (MoO_3) NPs showed good antibacterial properties against pathogenic bacteria [37].

In our previous studies, we have synthesized and examined properties of NCs based on epoxy resin and TiO_2 NPs surface modified with propyl, hexyl and lauryl gallate [38], as well as the influence of the size of TiO_2 nanoparticles, their concentration and type of the surface modification on the rheological properties of alkyd resin [28].

Since there is constantly increasing demand for developing environmentally friendly materials and taking into account that alkyd resins are one of the most applied resins and TiO_2 is one of the most applied pigment in coating industry, in the present study we have made an effort to prepare novel alkyd-based NCs with improved properties, by utilizing differently surface modified TiO_2 NPs and alkyd resin based on vegetable oil. Different types of ligands, grafted on the surface of TiO_2 NPs, were applied in order to improve interactions between

NPs and polymer matrix and consequently to enhance the properties of the alkyd-based coatings.

In the present study we have used TiO_2 NPs surface modified with hexyl (C6), lauryl (C12) and cetyl (C16) gallate, and imine obtained from 3,4-dihydroxybenzaldehyde and oleylamine to prepare novel soy alkyd-based NCs. The TiO_2 NPs were synthesized using acid catalyzed hydrolysis of titanium isopropoxide. The average size and size distribution of the synthesized TiO_2 NPs were determined by transmission electron microscopy (TEM), their crystal structure was investigated by X-ray diffraction (XRD) measurements, while surface modified TiO_2 NPs were characterized using TEM, XRD, FTIR and UV/VIS spectroscopy. The amount of adsorbed molecules on the surface of TiO_2 NPs was determined by thermogravimetric analysis (TGA). The influence of the type of TiO_2 nanoparticles surface modification, as well as the length of hydrophobic part of gallates used for surface modification of TiO_2 nanoparticles, on the dispersion of TiO_2 NPs in alkyd resin and on the rheological properties of the prepared dispersions, as well as on the thermal, barrier and mechanical properties and chemical resistance of alkyd resin/TiO_2 NCs was investigated.

2. Experimental section

2.1. Materials

Titanium isopropoxide was purchased from TCI Europe N.V. (Zwijndrecht, Belgium). Gallic acid, 2-propanol, 1-hexanol, lauryl gallate (LG) and oleylamine (OA) were obtained from Sigma–Aldrich (Germany). Cetyl alcohol was obtained from Fluka (Switzerland), while 3,4-dihydroxybenzaldehyde (DHBA) from Acros Organics (Geel, Belgium). Alkyd resin (AR65), CHS-ALKYD S 653, based on soy bean oil (65% of oil) was obtained from Spolchemie (Ústí nad Labem, Czech Republic). Ca-octoate (10%), Co-octoate (4%) and Zr-octoate (15%) were purchased from Tikkurila Zorka (Šabac, Serbia) and used as driers. All chemicals were used as received without further purification.

2.2. Synthesis of TiO_2 colloid

The synthesis of TiO_2 colloid was performed by hydrolysis of titanium isopropoxide using the procedure described in the literature [39]. Briefly, 12.5 mL of titanium isopropoxide and 2.0 mL of 2-propanol were added into the dropping funnel and then the mixture was added to 75 mL of deionized water and vigorously stirred. White precipitate was formed during the hydrolysis. Within 10 min of the alkoxide addition, 0.57 mL of 65% nitric acid was added to the hydrolysis mixture. The mixture was stirred for 8 h at 80°C, allowing 2-propanol to evaporate. Using this procedure, approximately 70 mL of stable TiO_2 colloidal solution was obtained.

2.3. Synthesis of gallic acid esters

The synthesis of hexyl (HG) and cetyl gallate (CG) was performed by esterification of gallic acid using 1-hexanol and cetyl alcohol. The esterification of gallic acid by 1-hexanol was performed using the procedure described in the literature [40]. In the reaction flask (250 mL), connected to a Soxhlet apparatus containing 10 g of sodiumsulfate as a drying agent, 50 g of gallic acid, 136 g of 1-hexanol and 1 mL of sulfuric acid were added. 80 mL of extra 1-hexanol was used to fill Soxhlet apparatus. The reaction mixture was stirred with magnetic stirrer at 165°C for 8 h. During the reaction, formed water made azeotrope with 1-hexanol and it was captured by drying agent in Soxhlet apparatus. Then, the reaction mixture was placed in Rotavapor (BÜCHI 461, Switzerland) and 1-hexanol was distilled until the mixture of 75 wt% of hexyl gallate in 1-hexanol was obtained. In order to crystallize, the reaction mixture was poured with stirring into methylene chloride. After that, the prepared suspension was washed with water, and hexyl gallate was placed between two layers. The crude product was separated by filtration, washed with water and methylene chloride and dried at 60°C in vacuum oven.

The esterification of gallic acid by cetyl alcohol was performed using the similar procedure as procedure described in the literature for the synthesis of octyl gallate [40]. In the reaction flask (250 mL), connected to a mechanical stirrer, a nitrogen inlet, a contact thermometer and a condenser for vacuum distillation, 70.24 g of cetyl alcohol was placed. The flask was heated to 60°C, and then 10.24 g of gallic acid and 0.5 mL of H_2SO_4 were added into the flask. The reaction mixture was heated up to 160°C with stirring under a stream of nitrogen. The course of the reaction was controlled by the amount of the formed water. After 5 h, a reduced pressure (0.4 bar) was applied to the flask for 1 h. The reaction mixture was then slowly cooled down to 55°C. In another flask (500 mL), equipped with a mechanical stirrer and reflux condenser, 250 mL of petrol ether heated to

55°C was added. The reaction mixture was then slowly with stirring, added into petrol ether, heated to 60°C and left to cool down to the room temperature. The precipitate was separated by filtration, washed with petrol ether and then with water. The obtained precipitate was then placed into the flask and the alcohol residue was separated by distillation with water vapor. After that, cetyl gallate was recrystallized two times from the mixture petrol ether/benzene (50:50 vol.) and dried at 60°C in vacuum oven.

2.4. Modification of TiO_2 nanoparticles with gallates

For the surface modification of TiO_2 NPs, three gallates with different hydrophobic part length (hexyl, lauryl and cetyl gallate) were applied. Modification of TiO_2 NPs with gallates was done according to the procedure described in the literature [38]. The procedure for the surface modification of TiO_2 NPs with lauryl gallate will be briefly described here. 0.1136 g of LG was dissolved in the mixture of chloroform and methanol and then mixed with 10 mL of TiO_2 colloid solution in a separation funnel. After short vigorous shaking, a dark-red chloroform phase with TiO_2 NPs surface modified with LG (TiO_2-LG) separated from the upper aqueous phase. The obtained dark-red phase was drop-wise added to 100 times larger amount of methanol. Nanoparticles of TiO_2-LG separated as precipitate, which was then redispersed in chloroform.

2.5. Modification of TiO_2 nanoparticles with imine based on 3,4-dihydroxybenzaldehyde and oleylamine

The surface modification of TiO_2 NPs with imine obtained from DHBA and OA was performed in the following manner. In one flask (50 mL), 0.09 g of DHBA was dissolved in 8 mL of methanol using magnetic stirrer, while in another flask (50 mL), 0.5 mL of 70% OA was added into 20 mL of chloroform. Then, 5 mL of TiO_2 colloid solution, previously diluted with 25 mL of distilled water, was vigorously mixed with prepared solutions. After leaving the obtained solution overnight, a dark-orange phase containing TiO_2 NPs surface modified with imine (TiO_2-DHBAOA) separated from the upper aqueous phase. The obtained dark-orange phase was then slowly, with simultaneous mixing with the magnetic stirrer, drop-wise added into 100 times larger amount of methanol. Nanoparticles of TiO_2-DHBAOA separated as precipitate, which was then redispersed in chloroform.

2.6. Preparation of the alkyd based nanocomposites

Alkyd based NCs, containing 2 wt% of TiO_2 NPs (calculated with respect to the total mass of solid mater in alkyd resin), were prepared by adding adequate amount of TiO_2 NPs surface modified with HG (TiO_2-HG), LG (TiO_2-LG), CG (TiO_2-CG) and DHBAOA (TiO_2-DHBAOA) dispersed in chloroform into AR65. So prepared mixtures were then mixed in ultrasonic bath (Sonorex Digitec, BANDELIN electronic GmbH & Co KG, Berlin, Germany) for 10 min. After that, chloroform was evaporated at room temperature under the reduced pressure. Then, in the reaction mixtures were added 50 wt% of white spirit (oil thinner), calculated with respect to the total mass of solid mater in alkyd resin, and adequate amount of driers (Table 1). In order to obtain completely cured NC films (AR65/TiO_2-HG, AR65/TiO_2-LG, AR65/TiO_2-CG and AR65/TiO_2-DHBAOA), the dispersions were drawn on two glass plates (10×10 cm and 15×20 cm) using wire-wound rods and then cured at room temperature for 21 days. Film based on the pure alkyd resin was obtained in the same manner.

2.7. Characterization of unmodified and surface modified TiO_2 nanoparticles

Transmission electron microscopy (JEOL-1200EX, Jeol Ltd. Tokyo, Japan) was applied to determine the average size of TiO_2 NPs, while the size distribution of TiO_2 NPs was obtained using Image J software. TEM images of surface modified TiO_2 NPs were recorded on JEM-1400 (Jeol Ltd. Tokyo, Japan). The X-ray powder diffraction measurements of unmodified and modified TiO_2 nanoparticles were performed on a Philips 1050 X-ray powder diffractometer (Philips, Netherlands) using Ni-filtered Cu Kα radiation and Bragg-Brentano focusing geometry. The patterns were taken in the 10–90° 2θ range

Table 1. The amount of driers used for the cross-linking of alkyd resin based nanocomposites

Drier	Metal content [%]*
Solution of Ca-octoate	0.10
Solution of Co-octoate	0.04
Solution of Zr-octoate	0.15

*Calculated with respect to the content of alkyd resin

with the step of 0.05° and exposure time of 6 s per step. Using X-ray Line Profile Fitting Program (XFIT) with a Fundamental Parameters convolution approach to generate line profiles [41], the coherent domain sizes of the prepared samples were calculated. FTIR spectra of gallic acid esters, dry unmodified and modified TiO_2 NPs in the form of KBr pellets were recorder using a Bomem MB-102 (Quebec, Canada) FTIR spectrophotometer. The absorption spectra of unmodified and surface modified TiO_2 NPs were recorded on a Perkin-Elmer Lambda-5 UV-Vis (MA, USA) spectrometer. Using thermogravimetric analysis, performed on Setaram Setsys Evolution-1750 (SETARAM S.A. France, Caluire – France) instrument in dynamic argon atmosphere (flow rate 20 cm^3/min) at a heating rate of 10°C/min, the amount of molecules adsorbed on the surface of TiO_2 NPs was determined. Before TGA measurements, investigated samples were dried in vacuum oven at 60°C for 12 h.

2.8. Characterization of alkyd resin, dispersions of modified TiO_2 nanoparticles in alkyd resin and prepared nanocomposite coatings

Complex dynamic viscosity of pure AR65 and dispersions of surface modified TiO_2 NPs in AR65, prepared by dispersing 2 wt% of surface modified TiO_2 NPs in AR65 using ultrasound, was determined on rheometer Rheometrics RMS 605 (Rheometric Scientific, Piscataway NJ, USA). Dynamic shear experiments were performed between cone and plate, at constant temperature of 25°C. The frequency was changed between 0.1 and 100 rad/s, at strain of 5%.

The dispersion of surface modified TiO_2 nanoparticles in alkyd matrix was investigated by Scanning Electron Microscopy (SEM) using JEOL JSM-6610LV (Jeol Ltd. Tokyo, Japan). In order to observe the cross section of the nanocomposite films, the piece of each examined sample was immersed in liquid nitrogen for 20 s, removed and immediately broken.

Differential scanning calorimetry (DSC) measurements were done on Q1000 (TA Instruments, USA) instrument in a nitrogen atmosphere, at a heating rate of 20°C/min. Thermooxidative stability of samples was determined by TGA (Setaram Setsys Evolution-1750) in air atmosphere (flow rate 25 cm^3/min), at a heating rate of 10°C/min.

Water vapour transfer rate (*WVTR*) through the prepared films was determined according to the method described in the standard ASTM:D1653 using BYK-Gardner permeability cup (BYK-Gardner GmbH, Geretsried, Germany), filled with a desiccant (dry calcium chloride). The investigated films were clamped and sealed across the open end of the cup and then the cup was placed in an atmosphere of controlled relative humidity (85%), which was provided by saturated potassium chloride solution. During measurements, vapour passes from a solution through the film to a desiccant within the permeability cup. Three *WVTR* measurements were performed for each investigated film and the average value is reported.

Tensile properties of the prepared samples were examined on Shimadzu Universal Testing Machine AG-Xplus (Shimadzu, Kyoto, Japan) with deformation rate of 5 mm/min using 100 N cell. Investigated specimens were cut from the dried films. For each sample the average value of five measurements was taken.

Using the non-destructive ultrasound thickness meter Posi Tector 200 (DeFelsko, USA), the thickness of dried films was calculated as average value of three measurements. The estimated thickness of the prepared dried films was 40±3 μm. The surface hardness of dried films was determined using König pendulum (Elcometer Pendulum Hardness Tester 3034, Elcometer Limited, Manchester, England). König pendulum hardness, expressed in seconds as average value of three measurements, was measured using films drawn on glass plates (10×10 cm).

Impact resistance of prepared films was determined according to the standard ASTM D 2794 using Erichsen Impact Tester, Model 304 (Hemer, Germany). The indentation was performed through the uncoated side of metal plate, i.e. the examined coating was exposed to convex deformation (extrusion). For each sample, five specimens were tested and their average has been reported. Adhesion of films coated on mild steel panels was determined by cross-cut (ISO 2409) test. For each film, three specimens were tested by cross-cut method and their average has been reported. Abrasion resistance of prepared films was determined by Taber Abraser Testing Apparatus (Taber Industries, USA) using No. CS-17 Resilent Calibrase Wheels in accordance with standard ASTM D 4060. Load applied to the abrasive wheels was

1000 g. For each film, three specimens were tested and their average has been reported.

The gel content of the prepared films was determined by immersion of square specimens (1.2×2.5 cm), placed in holder made from steel network, in xylene for 14 days, at room temperature. After that, test specimens were dried in vacuum oven at 100°C for 2 hours and then, their weight (w) was measured. Data of three different specimens of each investigated film were averaged. The gel content of the samples was calculated using the following Equation (1):

$$Gel\% = \frac{w}{w_0} \cdot 100 \quad (1)$$

where w_0 is the weight of the sample before immersion in xylene.

The chemical resistance of the prepared films to distilled water, 1M HCl, 0.15% NaOH, 3% NaCl, ethanol, acetone and sunflower oil was investigated using films drawn on glass plates (10×10 cm). Solvent was dripped on the examined film using Pasteur pipette and appearance of the film was observed during 24 hours. Three specimens of each film were tested. The obtained results are presented as time needed to reach certain change in the appearance of the examined films: (0) completely unaffected, (1) unaffected, slightly color changed, (2) film swelled and (3) film cracked.

3. Results and discussion

3.1. Properties of unmodified and surface modified TiO_2 nanoparticles

TEM image of TiO_2 NPs, prepared by acid catalyzed hydrolysis of titanium isopropoxide, is given in Figure 1. It can be observed that synthesized TiO_2 NPs have approximately spherical shape and average diameter of 3.9±0.9 nm. The crystal structure and average crystalline size of TiO_2 NPs were determined by XRD measurements and obtained X-ray diffraction patterns are given in Figure 2. It can be seen that synthesized TiO_2 NPs have anatase crystal form and it has been estimated that their coherent domain size is around 3.6 nm, which is in good agreement with TEM result.

According to the literature, TiO_2 NPs have on their surface some Ti atoms which are not in octahedral, but in square-pyramidal position [42]. The coordination number of such Ti atoms is therefore five and not six, and one of these five bonds between Ti and oxygen is shorter than others. Due to that, Ti atoms on the surface of TiO_2 NPs are more reactive than bulk ones and can react quite fast with hydroxyl groups of modifying agent, bonding in this manner the missing oxygen and leading to the formation of charge transfer (*CT*) complex. This process leads simultaneously to the formation of stable crystal anatase form, where coordination number of Ti atoms is six and all Ti–O bonds are of the same length.

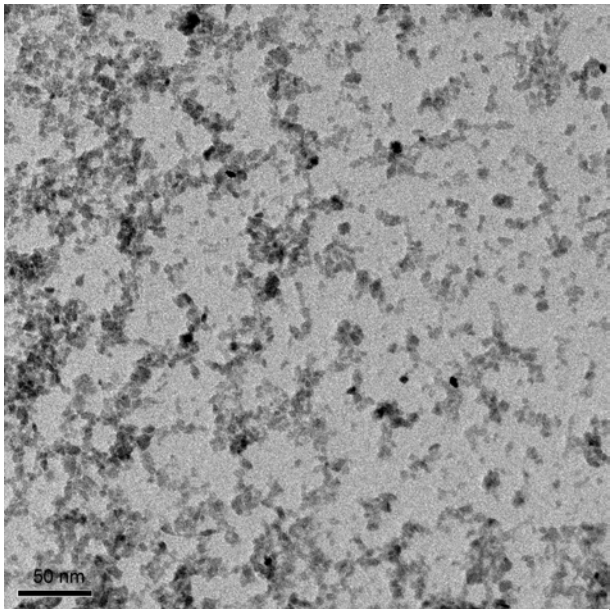

Figure 1. TEM image of TiO_2 nanoparticles

The surface modification of nanosized TiO_2 colloids was performed with three alkyl gallates with different hydrophobic part length (hexyl, lauryl and cetyl gallate) and with imine obtained from 3,4-dihydrox-

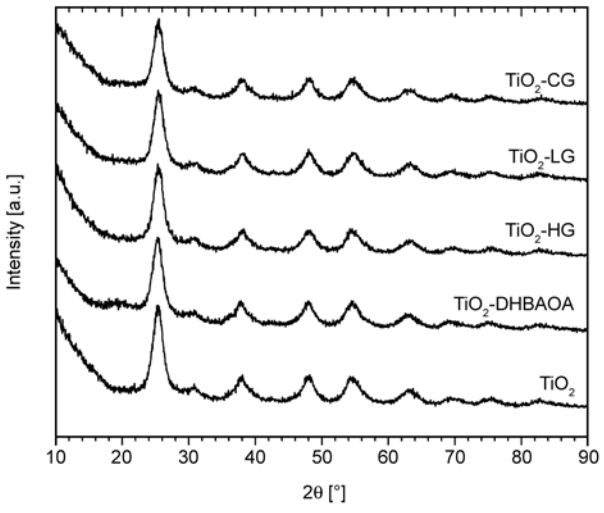

Figure 2. XRD patterns of unmodified and surface modified TiO_2 NPs

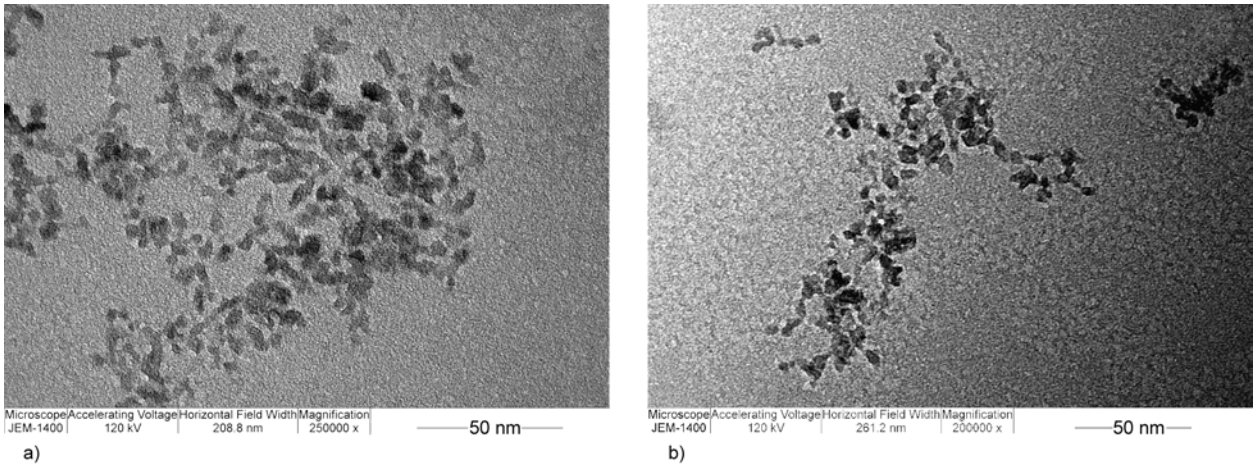

Figure 3. TEM images of TiO_2 nanoparticles surface modified with a) lauryl gallate and b) DHBAOA

ybenzaldehyde and oleylamine. During the modification process, a dark-red (when gallates were used for the modification) or dark-orange phase (when DHBAOA was used for the surface modification) separated, and transfer of NPs from water into organic phase occurred as a consequence of the formation of *CT* complex between TiO_2 NPs and gallates or DHBAOA. XRD patterns of modified TiO_2 NPs presented in Figure 2 show that the crystal structure and crystallite size of TiO_2 NPs were not changed by modification of TiO_2 NPs with gallates or DHBAOA, which was also confirmed by TEM analysis of modified TiO_2 NPs, reported in Figure 3. From the TEM analysis it can be observed that the morphology of TiO_2 NPs has not been changed during their surface modification.

The formation of *CT* complex between TiO_2 NPs and gallates or DHBAOA was confirmed by FTIR and UV-Vis spectroscopy. As an example, FTIR spectra of CG, dry TiO_2 colloid, dry TiO_2-CG, TiO_2-LG and TiO_2-HG NPs are presented in Figure 4a. From Figure 4a it can be observed that characteristic bands of CG at 3450 and 3350 cm^{-1}, which represent the stretching vibrations of –OH groups from benzene ring, are not present in the FTIR spectrum of TiO_2-CG NPs. On the other hand, the bands corresponding to the stretching vibration of aliphatic C–H bonds from cetyl group at 2920 and 2850 cm^{-1} and band which is assigned to the stretching vibration of C=O group from ester at 1670 cm^{-1} are also visible in the FTIR spectrum of TiO_2-CG NPs. According to these results, it can be concluded that the coordinative bond between surface Ti atoms and gallate was achieved through the adjacent –OH groups from the benzene ring, by creating bridging complexes, which is in agreement with our previous results [28,

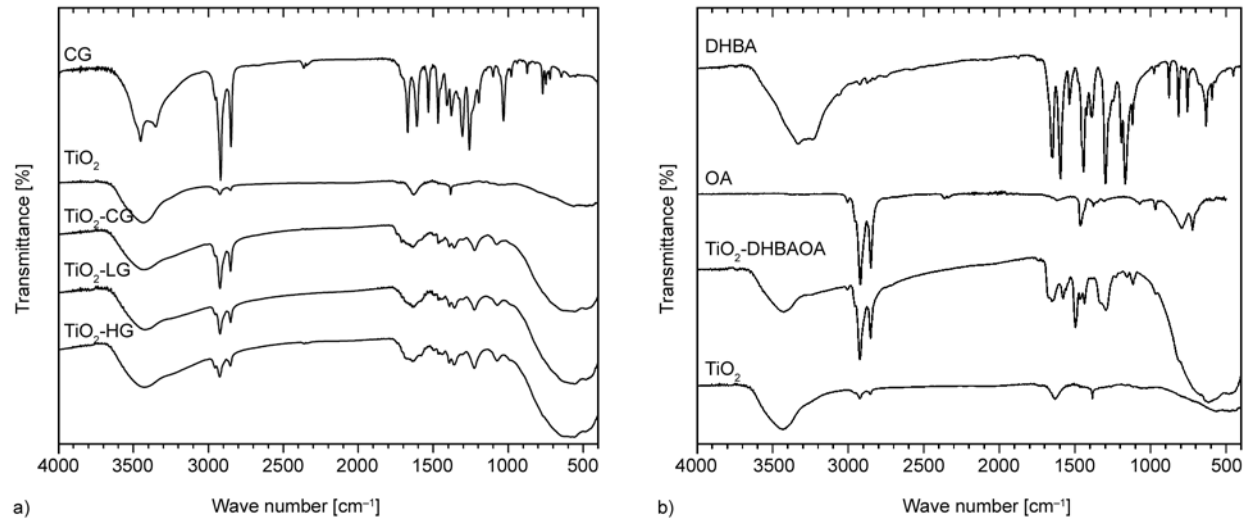

Figure 4. FTIR spectra of a) CG, dry TiO_2 colloid, dry TiO_2-CG, TiO_2-LG and TiO_2-HG NPs and b) OA, DHBAOA, dry TiO_2 colloid and TiO_2 NPs surface modified with DHBAOA

38, 43]. As can be observed from Figure 4a, similar results were obtained for the TiO_2-HG and TiO_2-LG NPs. Detailed explanation of the FTIR spectra of TiO_2 NPs surface modified with gallates is given elsewhere [38].

FTIR spectra of DHBA, OA, dry TiO_2 colloid and dry TiO_2-DHBAOA NPs are presented in Figure 4b. In the FTIR spectrum of TiO_2-DHBAOA, the bands at 3331 and 3233 cm^{-1}, assigned to the stretching vibrations of aldehyde phenolic –OH groups, and bands at 1389 and 1192 cm^{-1}, corresponding to the bending vibrations of phenolic –OH groups, are missing. Furthermore, the intensity of band at 1296 cm^{-1} (originating from the C–O stretching vibrations of phenolic group) is noticeable reduced, and the band became broader. Also, in the FTIR spectrum of TiO_2-DHBAOA, the band at 1576 cm^{-1}, assigned to the stretching vibrations of aromatic ring, and band at 1645 cm^{-1}, corresponding to the C=N stretching vibrations, are also visible. Furthermore, characteristic bands of the OA residue between 3000 and 2800 cm^{-1}, assigned to the asymmetric and symmetric C–H stretching vibrations of methyl and methylene groups, and at 3005 cm^{-1}, assigned to the C–H stretching vibrations in C=C–H group can also be observed. These results show that imine based on DHBA and OA was obtained and it was chemisorbed on TiO_2 surface through the two adjacent –OH phenolic groups of the aldehyde residue.

Absorption spectra of unmodified TiO_2 NPs and TiO_2 NPs surface modified with CG and DHBAOA

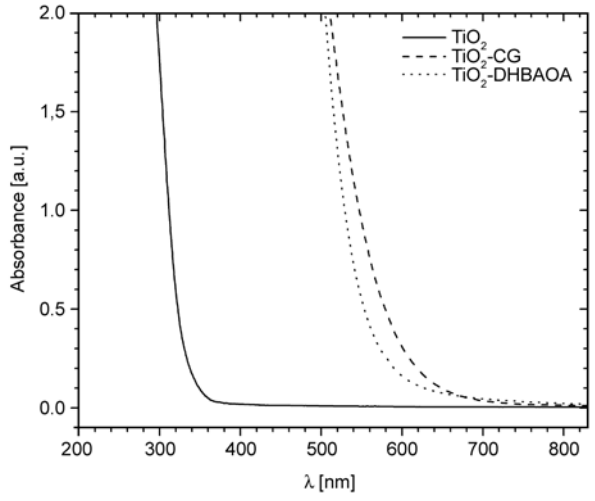

Figure 5. The absorption spectra of aqueous TiO_2 colloid solution and solutions of TiO_2-CG and TiO_2-DHBAOA in chloroform

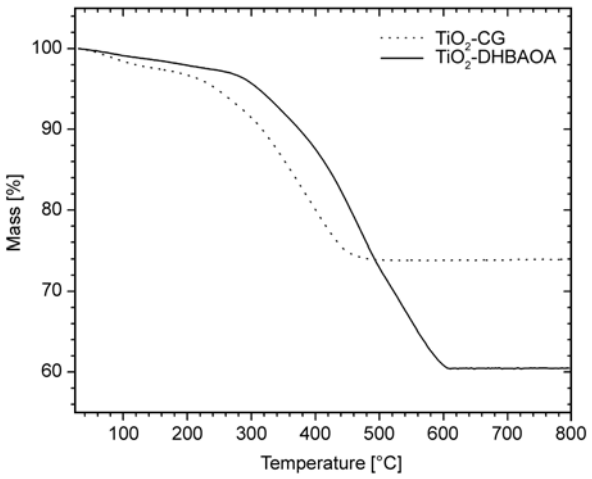

Figure 6. TGA curves of TiO_2-CG and TiO_2-DHBAOA NPs, obtained in argon atmosphere at a heating rate of 10°C/min

are shown in Figure 5. It can be observed that compared to the absorption spectrum of unmodified TiO_2 NPs, absorption spectra of surface modified TiO_2 NPs are red shifted, due to the CT complex formation on the surface of TiO_2 NPs. The absorption onset of unmodified, gallate and imine modified TiO_2 NPs is around 380, 640 and 610 nm, respectively.

In order to determine the amount of gallates and DHBAOA adsorbed on the surface of TiO_2, TGA measurements in argon atmosphere were performed. As an example, TGA curves of TiO_2-CG and TiO_2-DHBAOA are presented in Figure 6. It can be observed that thermal stability of TiO_2-DHBAOA NPs is higher than thermal stability of TiO_2-CG NPs. The first stage of thermal degradation of surface modified TiO_2 NPs occurred due to the mass loss of the absorbed water, while the second stage between 210 and 800°C corresponds to the mass loss of adsorbed ligand grafted on the surface of TiO_2 NPs. In our previous work we have shown that theoretical amount of adsorbed ligand necessary to cover all Ti surface sites should be 1.86 mmol of ligand per gram of TiO_2 [38]. According to the TGA results obtained here, the amount of the adsorbed ligands, TiO_2-HG, TiO_2-LG, TiO_2-CG and TiO_2-DHBAOA, are 0.90, 0.89, 0.80 and 1.53 mmol per gram of TiO_2, respectively. Consequently, the calculated coverage is for the TiO_2 NPs surface modified with gallates similar between each other (48% for TiO_2-HG and TiO_2-LG, and 43% for TiO_2-CG), while the amount of DHBAOA adsorbed on the surface of TiO_2 NPs is 82%.

3.2. Rheological properties of prepared dispersions of alkyd resin/TiO_2

The influence of surface modified TiO_2 NPs on the rheological properties of alkyd resin was investigated by measuring the dependence of complex dynamic viscosity (η^*) on frequency. From the results presented in Figure 7 it can be observed that prepared dispersions have higher dynamic viscosity than pure AR65 and that η^* decreases with increasing frequency for all investigated samples. Dynamic viscosity of the prepared dispersions depends on the interactions between surface modified TiO_2 NPs, as well as on the interactions between NPs and alkyd resin. Furthermore, from the samples prepared using TiO_2 NPs surface modified with gallates, the AR65/TiO_2-CG dispersion has the highest η^* value. This was reasonable to expect since TiO_2-CG NPs have the highest effective diameter. On the other hand, the viscosity of alkyd resin increased more after addition of TiO_2-HG than after addition of TiO_2-LG NPs. This indicates that TiO_2-HG NPs have low dispersion stability, leading to the formation of agglomerates in AR65, which are actually the main cause for the viscosity increase. Figure 7 also reveals that AR65/TiO_2-DHBAOA dispersion has the lowest η^* value from the investigated samples, indicating lower hydrodynamic radius of TiO_2-DHBAOA in AR65 than TiO_2 NPs surface modified with gallic acid esters.

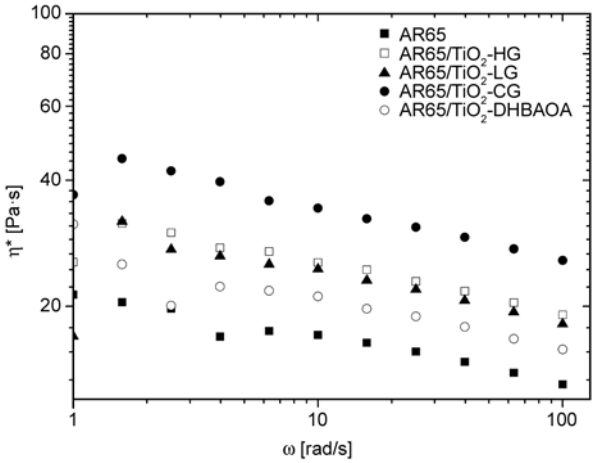

Figure 7. Frequency dependence of complex dynamic viscosity (η^*) for pure AR65 and AR65/TiO_2-HG, AR65/TiO_2-LG, AR65/TiO_2-CG and AR65/TiO_2-DHBAOA dispersions

3.3. SEM image analysis of cross-sections of the nanocomposite coatings

The cross-section of the prepared nanocomposite coatings was investigated by SEM analysis in order to examine the dispersion of surface modified TiO_2 NPs in polymer matrix. The SEM micrographs presented in Figure 8 show that TiO_2 NPs formed agglomerates in alkyd resin. Furthermore, it can be observed that agglomeration is more pronounced in NCs prepared with TiO_2 NPs surface modified with gallates and that formed agglomerates have approximately the same size no matter which ester of the gallic acid was used for the surface modification of TiO_2 NPs. The presence of agglomerates can also be observed in AR65/TiO_2-DHBAOA nanocomposite (Figure 8d and 8f), but their size is smaller and they are better dispersed in alkyd resin.

3.4. Thermal properties of AR65/TiO_2 nanocomposites

Glass transition temperature (T_g) of the synthesized NCs was determined using DSC measurements and obtained results are given in Figure 9 and summarized in Table 2. Furthermore, it can be observed that T_g of all investigated NCs is lower than T_g of pure AR65, which indicates that the presence of surface modified TiO_2 NPs increased molecular mobility of polymer chains at the polymer/nanoparticles interface, due to the absence of the attractive interactions between NPs and polymer matrix. The increase of the hydrophobic part length of the used

Table 2. Values of the glass transition temperature (T_g), water vapour transfer rate (*WVTR*), modulus of elasticity (E), stress at break (σ_B) and strain at break (ε_B) of the pure alkyd resin and prepared nanocomposites (*WVTR* values were determined as average value of three measurements, while tensile properties were determined as average value of five measurements and all results are reported with a standard deviation)

Sample	T_g [°C]	*WVTR* [g/(m²·h)]	E [MPa]	σ_B [MPa]	ε_B [%]
AR65	25	3.80±0.20	354±14	12.3±0.86	39.1±5.80
AR65/TiO_2-HG	21	2.68±0.11	279±8	13.1±1.00	47.6±5.71
AR65/TiO_2-LG	23	3.44±0.21	144±6	14.0±1.12	53.7±9.12
AR65/TiO_2-CG	23	3.40±0.18	246±12	11.9±0.71	45.8±4.72
AR65/TiO_2-DHBAOA	20	3.66±0.23	124±5	12.5±1.12	62.3±9.34

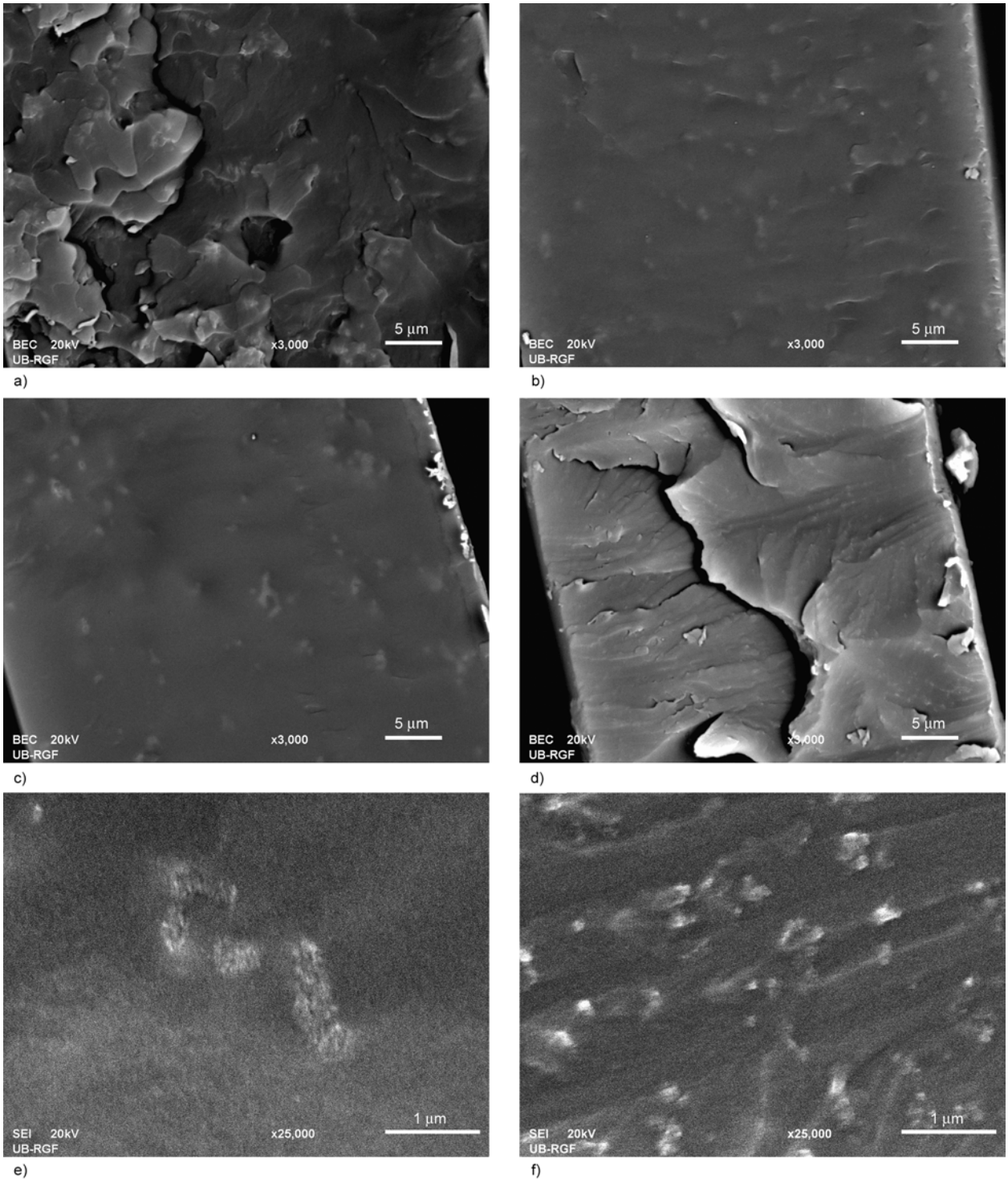

Figure 8. SEM micrographs of the cross-section of a) AR65/TiO_2-HG, b) AR65/TiO_2-LG, c) AR65/TiO_2-CG, d) AR65/TiO_2-DHBAOA at magnification of 3000×, and e) AR65/TiO_2-CG and f) AR65/TiO_2-DHBAOA at magnification of 25000×

gallic acid esters led to only slight increase of the T_g of prepared NCs.

The influence of differently surface modified TiO_2 NPs on thermooxidative stability of alkyd resin was investigated by TGA under air atmosphere, at a heating rate of 10°C/min. The results presented in Figure 10 show that thermooxidative degradation of all investigated samples took place in two stages, first at around 350°C and second at around 450°C. The first stage of thermooxidative degradation can be ascribed to the thermal degradation of polyester part of the alkyd resin chains, while the second stage occurred as a consequence of degradation of fatty acids chains [44]. The presence of surface modified

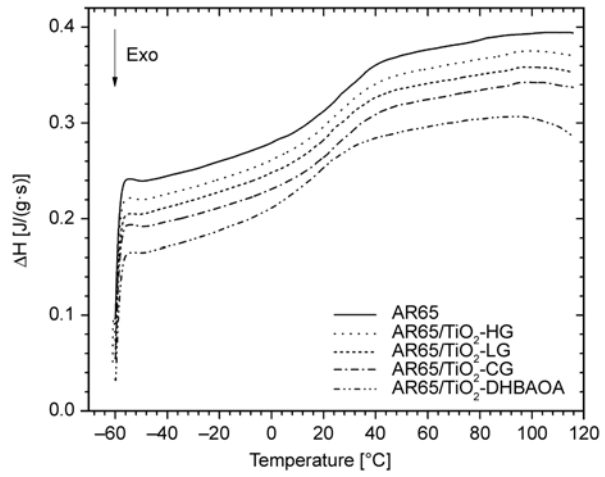

Figure 9. DSC curves of pure AR65 and AR65/TiO_2-HG, AR65/TiO_2-LG, AR65/TiO_2-CG and AR65/TiO_2-DHBAOA nanocomposites

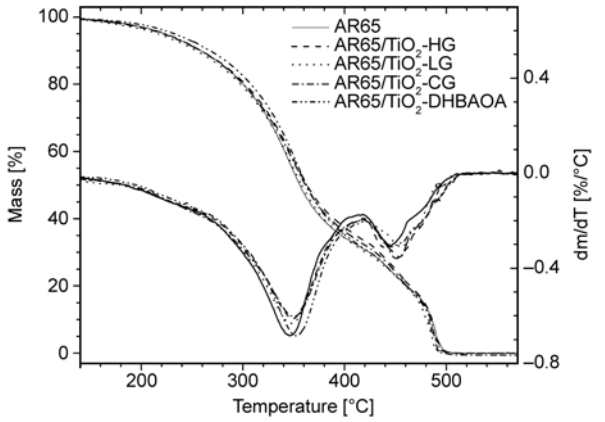

Figure 10. TGA and DTG curves of pure AR65 and AR65/TiO_2-HG, AR65/TiO_2-LG, AR65/TiO_2-CG and AR65/TiO_2-DHBAOA nanocomposites determined in air atmosphere at a heating rate of 10°C/min

TiO_2 NPs in AR65 shifted the position of both derivative thermogram (DTG) peaks to slightly higher temperatures compared to the DTG peaks of pure alkyd resin. This improvement of thermooxidative stability was more pronounced for AR65/TiO_2-DHBAOA during the first stage of degradation than for other investigated nanocomposites.

3.5. Barrier properties of AR65/TiO_2 nanocomposites

The cross-linking density of long oil alkyd resin is usually not enough to reduce diffusivity of permeating molecules through the prepared coating. On the other hand, the filler particles, compatible with polymer matrix and well dispersed in it, can be applied as good strategy to improve barrier properties of organic

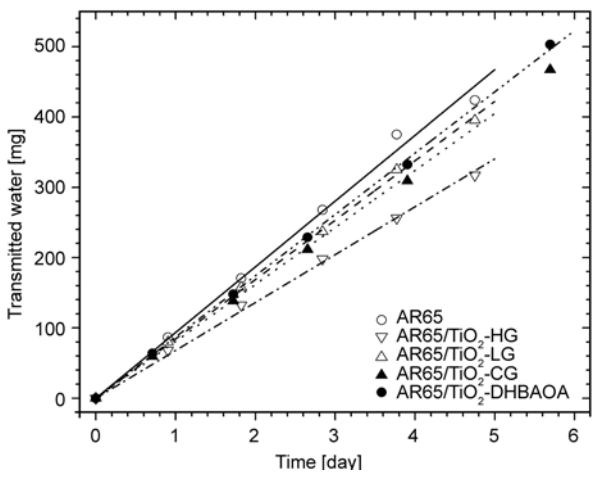

Figure 11. The dependence of the transmitted water through the pure AR65 and prepared nanocomposites on time

coatings [45–47]. The presence of NPs enhances the degree of tortuosity of the permeating molecules diffusion path through the polymer, by occupying the free volume within the polymer. Therefore, the water vapour barrier properties of the alkyd resin and prepared NCs were investigated by water vapour permeability measurements. Obtained results are presented in Figure 11 and listed in Table 2. According to these results it can be concluded that the presence of TiO_2 NPs surface modified with gallates and DHBAOA reduces *WVTR* of alkyd resin, whereby AR65/TiO_2-HG NC has the lowest *WVTR* value. Therefore, prepared NCs can be applied as efficient protection coating against corrosion of metal surfaces.

3.6. Tensile properties of AR65/TiO_2 nanocomposites

The stress-strain curves of pure alkyd resin and prepared NCs are given in Figure 12. From these results, values of the modulus of elasticity (E), stress at break (σ_B) and strain at break (ε_B) of the pure alkyd resin and prepared nanocomposites were determined and listed in Table 2. Modulus of elasticity of AR65 is higher than the value obtained for the prepared NCs, indicating that pure alkyd resin is stiffer than other investigated samples. Simultaneously, alkyd resin has also the lowest value of strain at break. The rigidity of the commercial alkyd resin originates from the presence of polyesters chains in its structure. On the other hand, the low value of strain at break comes from the relatively fast curing of alkyd resin, despite the presence of certain flexibility from

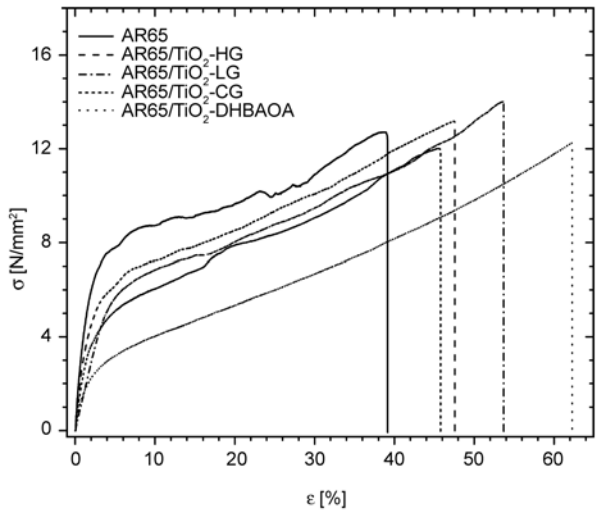

Figure 12. The dependence stress-strain of pure AR65 and AR65/TiO_2-HG, AR65/TiO_2-LG, AR65/TiO_2-CG and AR65/TiO_2-DHBAOA nanocomposites

fatty acids chains [48]. The stress-strain curves given in Figure 12 also show that tensile properties of prepared AR65/TiO_2 NCs are dependent on the type of NPs surface modification. After addition of surface modified TiO_2 NPs into AR65, the largest decrease in modulus and increase in strain at break was observed for AR65/TiO_2-DHBAOA nanocomposite, which is consistent with the lowest T_g value obtained for this NC. Furthermore, the increase of the gallates alkyl chain length from 6C (hexyl gallate) to 12C (lauryl gallate) induced lower E and higher σ_B and ε_B values. In contrast, further increase of the hydrophobic part length of the used gallic acid esters to 16C (cetyl gallate) led to increase of the modulus of elasticity and decrease of the stress and strain at break. The obtained results revealed that stiffness of the alkyd resin based on soy bean oil can be reduced by addition of 2 wt% of TiO_2 NPs surface modified with gallates, simultaneously leading to the formation of NC with relatively high values of σ_B and ε_B. The highest impact on the increase of stress at break was observed after addition of TiO_2-LG NPs into the AR65.

3.7. Mechanical properties of AR65/TiO_2 nanocomposite coatings

The hardness of the prepared coatings was determined using König pendulum. From the obtained results, listed in Table 3, it can be observed that addition of TiO_2 NPs surface modified with gallic acid esters leads to the increase of surface hardness (König hardness) of the alkyd resin, while with increasing alkyl chain length of the applied gallate hardness decreased. The certain increase of the surface hardness of air dried alkyd coatings by addition of colloidal SiO_2 particles was also observed by Kurt *et al.* [49]. Furthermore, Bal and coworkers [50, 51] have found that NC coatings based on alkyd-melamine formaldehyde resin and modified silica, as well as films prepared from alkyd-phenol formaldehyde resin and organo clay have higher König hardness than pure resin. On the other hand, obtained results revealed that AR65/TiO_2-DHBAOA has slightly lower value of the König hardness than pure alkyd resin. The probable reason for such behavior could be the lowest cross-linking density of this sample. This NC sample has the lowest T_g, the lowest modulus of elasticity and the highest strain at break. Also, it has better dispersion of nanofiller in polymer matrix than other NCs. Furthermore, AR65/TiO_2-DHBAOA had the highest concentration of unsaturated double bonds before curing (additional double bounds originating from DHBAOA ligands), causing faster curing reaction, which can lead to the lower cross-linking density of cured sample. All this implies that this sample has the lowest cross-linking density and that was the reason why it showed the opposite behavior compared to the other NCs.

From the results listed in Table 3 it can be observed that impact strength of all investigated samples is

Table 3. Values of the König hardness, impact strength, adhesion and abrasion resistance of the pure alkyd resin and prepared nanocomposites (König hardness, adhesion and abrasion resistance were determined as average value of three measurements, while impact strength as average value of five measurements and values of König hardness and abrasion resistance are reported with a standard deviation) 80 in-lb corresponds to 9 J

Sample	König hardness [s]	Impact strength [in-lb]	Adhesion resistance (ISO 2409)	Abrasion resistance (wear index)
AR65	31±1	>80	Gt 0	103±10
AR65/TiO_2-HG	38±2	>80	Gt 0	140±11
AR65/TiO_2-LG	34±2	>80	Gt 0	109±9
AR65/TiO_2-CG	33±2	>80	Gt 0	121±10
AR65/TiO_2-DHBAOA	28±1	>80	Gt 0	115±12

larger than 80 in-lb (9 J), indicating good flexibility of the prepared coatings. Furthermore, adhesion resistance of the prepared coatings was determined according to the ISO 2409 standard and obtained results listed in Table 3 indicate that all examined coatings have very good adhesion to the metal substrate. The results of the abrasion resistance test of examined coatings are shown in Table 3. It could be seen that the wear index is higher for NC coatings, indicating the deterioration of abrasion resistance of alkyd coatings after addition of surface modified TiO_2 nanoparticles. It is well known that the quality of the interface between NPs and polymer matrics defines material capability to transfer stresses and elastic deformation from the polymer matrix to the nanofillers. According to the DSC results, NCs prepared in this work have lower T_g than pure alkyd resin, indicating the poor interaction between NPs and polymer matrix at the interface. Therefore, NPs are not able to bear the applied load and due to that the abrasion resistance of NCs cannot be better than that of the pure polymer matrix [52].

3.8. Gel content and chemical resistance of AR65/TiO_2 nanocomposite coatings

The gel content of the prepared films was determined according to the procedure described in the experimental section and obtained results are listed in Table 4. It can be observed that all examined samples have approximately the same gel content, which indicates that the presence of surface modified TiO_2 NPs has no significant influence on the content of residual soluble components.

The results of the chemical resistance investigation of the pure AR65 and prepared nanocomposite coatings are given in Table 4. All examined samples show good resistance to distilled water, 1M HCl, 3% NaCl and sunflower oil and after 24 hours there was no change in the appearance of the examined coatings. Furthermore, nanocomposite coatings showed better resistance to 0.15% NaOH, acetone and ethanol than pure alkyd resin, but after certain time all NC films cracked.

4. Conclusions

Novel soy alkyd-based nanocomposite coatings were synthesized using TiO_2 NPs surface modified with hexyl, lauryl and cetyl gallate, and imine obtained from 3,4-dihydroxybenzaldehyde and oleylamine. Anatase TiO_2 NPs (average diameter of 3.9±0.9 nm) were prepared via acid catalyzed hydrolysis of titanium isopropoxide. FTIR and UV-Vis spectroscopy confirmed surface modification of TiO_2 NPs. Furthermore, TEM and XRD analysis revealed that morphology, crystal structure and crystallite size of TiO_2 NPs were not changed by surface modification of TiO_2 NPs, while the amount ligands adsorbed on the surface of TiO_2 NPs was calculated from TGA measurements. Experimental results presented in this work further demonstrated:

– Dynamic viscosity of AR65/TiO_2 dispersions is higher than for pure AR65 and it decreases with increasing frequency. AR65/TiO_2-DHBAOA dispersion exhibited the lowest η^* value, due to the lower hydrodynamic radius of TiO_2-DHBAOA NPs in AR65 than TiO_2 NPs surface modified with gallates.
– SEM analysis of the prepared NC coatings showed that surface modified TiO_2 NPs formed agglomerates in alkyd resin and that the size of TiO_2-

Table 4. The gel content and chemical resistance investigation of the pure alkyd resin and prepared nanocomposites (three specimens of each film were tested; gel content is reported with a standard deviation)

Solvent	AR65	AR65/TiO_2-HG	AR65/TiO_2-LG	AR65/TiO_2-CG	AR65/TiO_2-DHBAOA
Gel% [%]	88.8±1.8	89.1±2.0	88.9±1.9	89.8±2.1	87.0±1.9
Distilled water	24 h (0)	24 h (0)	24 h (0)	24 h (0)	24 h (0)
1M HCl	24 h (0)	24 h (0)	24 h (0)	24 h (0)	24 h (0)
0.15% NaOH	5 min (1) d*	10 min (1) d*	10 min (1) d*	10 min (1) d*	10 min (1) l*
	70 min (2)	70 min (2)	70 min (2)	70 min (2)	70 min (2)
	90 min (3)	90 min (3)	90 min (3)	90 min (3)	90 min (3)
3% NaCl	24 h (0)	24 h (0)	24 h (0)	24 h (0)	24 h (0)
Ethanol	21 min (3)	35 min (3)	36 min (3)	32 min (3)	37 min (3)
Acetone	13 s (3)	15 s (3)	22 s (3)	24 s (3)	28 s (3)
Sunflower oil	24 h (0)	24 h (0)	24 h (0)	24 h (0)	24 h (0)

(0) completely unaffected, (1) unaffected, slightly color changed, (2) film swelled and (3) film cracked
*d – the change of the film color to darker, l – the change of the film color to lighter

DHBAOA agglomerates is smaller than the size of agglomerates formed by TiO_2 NPs surface modified with gallates.

- T_g of prepared NCs is lower than T_g of pure alkyd resin, indicating the absence of attractive interactions between NPs and polymer matrix. The change of the hydrophobic part length of gallates showed no significant influence on the T_g of prepared NCs.
- The presence of TiO_2 NPs surface modified with gallates had no significant influence on the thermooxidative stability of AR65, while TiO_2-DHBAOA NPs induced slightly better thermooxidative stability.
- All examined samples have approximately the same gel content, which indicates that the presence of surface modified TiO_2 NPs has no significant influence on the cross-linking density of the alkyd resin.
- The presence of TiO_2 NPs surface modified with gallates and DHBAOA reduced *WVTR*, modulus of elasticity and abrasion resistance of alkyd resin and improved strain at break and chemical resistance. Furthermore, all prepared coatings have good flexibility and very good adhesion to the metal substrate, and addition of TiO_2 NPs surface modified with gallates increased surface König hardness of the alkyd resin, while the presence of TiO_2-DHBAOA NPs had no significant influence on it.

Acknowledgements

This work was financially supported by the Ministry of Education, Science and Technological Development of the Republic of Serbia (research project number: 172062).

References

[1] Hofland A.: Alkyd resins: From down and out to alive and kicking. Progress in Organic Coatings, **73**, 274–282 (2012).
DOI: 10.1016/j.porgcoat.2011.01.014

[2] Deligny P., Tuck N.: Resins for surface coatings: Alkyds and polyesters. Wiley, London (2000).

[3] Soucek M. D., Khattab T., Wu J.: Review of autoxidation and driers. Progress in Organic Coatings, **73**, 435–454 (2012).
DOI: 10.1016/j.porgcoat.2011.08.021

[4] Bal A., Güçlü G., Acar I., İyim T. B.: Effects of urea formaldehyde resin to film properties of alkyd–melamine formaldehyde resins containing organo clay. Progress in Organic Coatings, **68**, 363–365 (2010).
DOI: 10.1016/j.porgcoat.2010.03.006

[5] Alam M., Akram D., Sharmin E., Zafar F., Ahmad S.: Vegetable oil based eco-friendly coating materials: A review article. Arabian Journal of Chemistry, **7**, 469–479 (2014).
DOI: 10.1016/j.arabjc.2013.12.023

[6] Belgacem M. N., Gandini A.: Materials from vegetable oils: Major sources, properties and applications. in 'Monomers, polymers and composites from renewable resources' (eds.: Belgacem M. N., Gandini A.) Elsevier, Oxford, 39-66 (2008).

[7] Athawale V. D., Nimbalkar R. V.: Waterborne coatings based on renewable oil resources: An overview. Journal of the American Oil Chemists' Society, **88**, 159–185 (2011).
DOI: 10.1007/s11746-010-1668-9

[8] Güçlü G., Orbay M.: Alkyd resins synthesized from postconsumer PET bottles. Progress in Organic Coatings, **65**, 362–365 (2009).
DOI: 10.1016/j.porgcoat.2009.02.004

[9] Alidedeoglu A. H., Davis K., Robertson R., Smith C., Rawlins J. W., Morgan S. E.: Synthesis and evaluation of tetra(2,7-octadienyl) titanate as a reactive diluent for air-drying alkyd paints. Journal of Coatings Technology and Research, **8**, 45–52 (2011).
DOI: 10.1007/s11998-010-9276-z

[10] Atta A. M., El-Ghazawy R. A., El-Saeed A. M.: Corrosion protective coating based on alkyd resins derived from recycled poly (ethylene terephthalate) waste for carbon steel. International Journal of Electrochemical Science, **8**, 5136–5152 (2013).

[11] Ang D. T. C., Gan S. N.: Development of palm oil-based alkyds as UV curable coatings. Pigment and Resin Technology, **41**, 302–310 (2012).
DOI: 10.1108/03699421211264866

[12] Ataei S., Yahya R., Gan S. N.: Fast physical drying, high water and salt resistant coatings from non-drying vegetable oil. Progress in Organic Coatings, **72**, 703–708 (2011).
DOI: 10.1016/j.porgcoat.2011.07.013

[13] İşeri-Çağlar D., Baştürk E., Oktay B., Kahraman M. V.: Preparation and evaluation of linseed oil based alkyd paints. Progress in Organic Coatings, **77**, 81–86 (2014).
DOI: 10.1016/j.porgcoat.2013.08.005

[14] Boruah M., Gogoi P., Adhikari B., Dolui S. K.: Preparation and characterization of *Jatropha curcas* oil based alkyd resin suitable for surface coating. Progress in Organic Coatings, **74**, 596–602 (2012).
DOI: 10.1016/j.porgcoat.2012.02.007

[15] Bora M. M., Gogoi P., Deka D. C., Kakati D. K.: Synthesis and characterization of yellow oleander (*Thevetia peruviana*) seed oil-based alkyd resin. Industrial Crops and Products, **52**, 721–728 (2014).
DOI: 10.1016/j.indcrop.2013.11.012

[16] Araujo W. S., Margarit I. C. P., Mattos O. R., Fragata F. L., de Lima-Neto P.: Corrosion aspects of alkyd paints modified with linseed and soy oils. Electrochimica Acta, **55**, 6204–6211 (2010).
DOI: 10.1016/j.electacta.2010.03.088

[17] Atimuttigul V., Damrongsakkul S., Tanthapanichakoon W.: Effects of oil type on the properties of short oil alkyd coating materials. Korean Journal of Chemical Engineering, **23**, 672–677 (2006).
DOI: 10.1007/BF02706813

[18] Pathan S., Ahmad S.: s-triazine ring-modified waterborne alkyd: Synthesis, characterization, antibacterial, and electrochemical corrosion studies. ACS Sustainable Chemistry and Engineering, **1**, 1246–1257 (2013).
DOI: 10.1021/sc4001077

[19] Nalawade P. P., Mehta B., Pugh C., Soucek M. D.: Modified soybean oil as a reactive diluent: Synthesis and characterization. Journal of Polymer Science Part A: Polymer Chemistry, **52**, 3045–3059 (2014).
DOI: 10.1002/pola.27352

[20] Perera D. Y.: Effect of pigmentation on organic coating characteristics. Progress in Organic Coatings, **50**, 247–262 (2004).
DOI: 10.1016/j.porgcoat.2004.03.002

[21] Popa M. V., Drob P., Vasilescu E., Mirza-Rosca J. C., Santana Lopez A., Vasilescu C., Drob S. I.: The pigment influence on the anticorrosive performance of some alkyd films. Materials Chemistry and Physics, **100**, 296–303 (2006).
DOI: 10.1016/j.matchemphys.2006.01.002

[22] Bhavsar R., Raj R., Parmar R.: Studies of sedimentation behaviour of high pigmented alkyd primer: A rheological approach. Progress in Organic Coatings, **76**, 852–857 (2013).
DOI: 10.1016/j.porgcoat.2013.02.009

[23] Kamat P. V.: Photophysical, photochemical and photocatalytic aspects of metal nanoparticles. The Journal of Physical Chemistry B, **106**, 7729–7744 (2002).
DOI: 10.1021/jp0209289

[24] Bajpai O. P., Kamdi J. B., Selvakumar M., Ram S., Khastgir D., Chattopadhyay S.: Effect of surface modification of $BiFeO_3$ on the dielectric, ferroelectric, magneto-dielectric properties of polyvinylacetate/$BiFeO_3$ nanocomposites. Express Polymer Letters, **8**, 669–681 (2014).
DOI: 10.3144/expresspolymlett.2014.70

[25] Ju S., Chen M., Zhang H., Zhang Z.: Dielectric properties of nanosilica/low-density polyethylene composites: The surface chemistry of nanoparticles and deep traps induced by nanoparticles. Express Polymer Letters, **8**, 682–691 (2014).
DOI: 10.3144/expresspolymlett.2014.71

[26] Dhoke S. K., Bhandari R., Khanna A. S.: Effect of nano-ZnO addition on the silicone-modified alkyd-based waterborne coatings on its mechanical and heat-resistance properties. Progress in Organic Coatings, **64**, 39–46 (2009).
DOI: 10.1016/j.porgcoat.2008.07.007

[27] Dhoke S. K., Khanna A. S.: Study on electrochemical behavior of nano-ZnO modified alkyd-based waterborne coatings. Journal of Applied Polymer Science, **113**, 2232–2237 (2009).
DOI: 10.1002/app.30276

[28] Radoman T. S., Džunuzović J. V., Jeremić K. B., Marinković A. D., Spasojević P. M., Popović I. G., Džunuzović E. S.: The influence of the size and surface modification of TiO_2 nanoparticles on the rheological properties of alkyd resin (in Serbian). Hemijska Industrija, **67**, 923–932 (2013).
DOI: 10.2298/HEMIND131106081R

[29] Shi H., Liu F., Han E., Wei Y.: Effects of nano pigments on the corrosion resistance of alkyd coating. Journal of Materials Science and Technology, **23**, 551–558 (2007).

[30] Deyab M. A., Keera S. T.: Effect of nano-TiO_2 particles size on the corrosion resistance of alkyd coating. Materials Chemistry and Physics, **146**, 406–411 (2014).
DOI: 10.1016/j.matchemphys.2014.03.045

[31] Subbiah G., Premanathan M., Kim S. J., Krishnamoorthy K., Jeyasubramanian K.: Preparation of TiO_2 nanopaint using ball milling process and investigation on its antibacterial properties. Materials Express, **4**, 393–399 (2014).
DOI: 10.1166/mex.2014.1185

[32] Dhoke S. K., Khanna A. S.: Effect of nano-Fe_2O_3 particles on the corrosion behavior of alkyd based waterborne coatings. Corrosion Science, **51**, 6–20 (2009).
DOI: 10.1016/j.corsci.2008.09.028

[33] Dhoke S. K., Khanna A. S.: Electrochemical behavior of nano-iron oxide modified alkyd based waterborne coatings. Materials Chemistry and Physics, **117**, 550–556 (2009).
DOI: 10.1016/j.matchemphys.2009.07.010

[34] Rahman O. U., Ahmad S.: Physico-mechanical and electrochemical corrosion behavior of soy alkyd/Fe_3O_4 nanocomposite coatings. RSC Advances, 4, 14936-14947 (2014).
DOI: 10.1039/c3ra48068b

[35] Dhoke S. K., Khanna A. S.: Electrochemical impedance spectroscopy (EIS) study of nano-alumina modified alkyd based waterborne coatings. Progress in Organic Coatings, **74**, 92–99 (2012).
DOI: 10.1016/j.porgcoat.2011.11.020

[36] Dhoke S. K., Sinha T. J. M., Khanna A. S.: Effect of nano-Al_2O_3 particles on the corrosion behavior of alkyd based waterborne coatings. Journal of Coatings Technology and Research, **6**, 353–368 (2009).
DOI: 10.1007/s11998-008-9127-3

[37] Krishnamoorthy K., Premanathan M., Veerapandian M., Kim S. J.: Nanostructured molybdenum oxide-based antibacterial paint: Effective growth inhibition of various pathogenic bacteria. Nanotechnology, **25**, 315101/1–315101/10 (2014).
DOI: 10.1088/0957-4484/25/31/315101

[38] Radoman T. S., Džunuzović J. V., Jeremić K. B., Grgur B. N., Miličević D. S., Popović I. G., Džunuzović E. S.: Improvement of epoxy resin properties by incorporation of TiO_2 nanoparticles surface modified with gallic acid esters. Materials and Design, **62**, 158–167 (2014).
DOI: 10.1016/j.matdes.2014.05.015

[39] O'Regan B., Moser J., Anderson M., Graetzel M.: Vectorial electron injection into transparent semiconductor membranes and electric field effects on the dynamics of light-induced charge separation. The Journal of Physical Chemistry, **94**, 8720–8726 (1990).
DOI: 10.1021/j100387a017

[40] Coppens B., Sas B., van Hemel J.: Method of synthesizing alkyl gallates. WO2001030299 (2001).

[41] Cheary R. W., Coelho A.: A fundamental parameters approach to X-ray line-profile fitting. Journal of Applied Crystallography, **25**, 109–121 (1992).
DOI: 10.1107/S0021889891010804

[42] Rajh T., Nedeljković J. M., Chen L. X., Poluektov O., Thurnauer M. C.: Improving optical and charge separation properties of nanocrystalline TiO_2 by surface modification with vitamin C. The Journal of Physical Chemistry B, **103**, 3515–3519 (1999).
DOI: 10.1021/jp9901904

[43] Janković I. A., Šaponjić Z. V., Džunuzović E. S., Nedeljković J. M.: New hybrid properties of TiO_2 nanoparticles surface modified with catecholate type ligands. Nanoscale Research Letters, **5**, 81–88 (2010).
DOI: 10.1007/s11671-009-9447-y

[44] Ploeger R., Scalarone D., Chiantore O.: Thermal analytical study of the oxidative stability of artists' alkyd paints. Polymer Degradation and Stability, **94**, 2036–2041 (2009).
DOI: 10.1016/j.polymdegradstab.2009.07.018

[45] Shreepathi S., Naik S. M., Vattipalli M. R.: Water transportation through organic coatings: Correlation between electrochemical impedance measurements, gravimetry, and water vapor permeability. Journal of Coatings Technology and Research, **9**, 411–422 (2012).
DOI: 10.1007/s11998-011-9376-4

[46] Aulin C., Salazar-Alvarez G., Lindström T.: High strength, flexible and transparent nanofibrillated cellulose–nanoclay biohybrid films with tunable oxygen and water vapor permeability. Nanoscale, **4**, 6622–6628 (2012).
DOI: 10.1039/c2nr31726e

[47] Pavlacky E., Ravindran N., Webster D. C.: Novel *in situ* synthesis in the preparation of ultraviolet-curable nanocomposite barrier coatings. Journal of Applied Polymer Science, **125**, 3836–3848 (2012).
DOI: 10.1002/app.36716

[48] Wutticharoenwong K., Dziczkowski J., Soucek M. D.: Tung based reactive diluents for alkyd systems: Film properties. Progress in Organic Coatings, **73**, 283–290 (2012).
DOI: 10.1016/j.porgcoat.2011.03.017

[49] Kurt İ., Acar I., Güçlü G.: Preparation and characterization of water reducible alkyd resin/colloidal silica nanocomposite coatings. Progress in Organic Coatings, **77**, 949–956 (2014).
DOI: 10.1016/j.porgcoat.2014.01.017

[50] Bal A., Acar I., Güçlü G.: A novel type nanocomposite coating based on alkyd-melamine formaldehyde resin containing modified silica: Preparation and film properties. Journal of Applied Polymer Science, **125**, E85–E92 (2012).
DOI: 10.1002/app.35029

[51] Bal A., Acar I., Güçlü G., İyim T. B.: Effects of organo clay on film properties of alkyd-phenol formaldehyde resins. Pigment and Resin Technology, **41**, 100–103 (2012).
DOI: 10.1108/03699421211210757

[52] Kurahatti R. V., Surendranathan A. O., Srivastava S., Singh N., Ramesh Kumar A. V., Suresha B.: Role of zirconia filler on friction and dry sliding wear behaviour of bismaleimide nanocomposites. Materials and Design, **32**, 2644–2649 (2011).
DOI: 10.1016/j.matdes.2011.01.030